Deep Learning Applications in Histopathological Images

Luis Felipe Rocha Pereira[1(✉)], Anselmo Cardoso de Paiva[2,3], Alexandre de Carvalho Araújo[3], Geraldo Braz Junior[3], Joao Dallyson Sousa de Almeida[1,2,3], and Aristófanes Corrêa Silva[1,2,3]

[1] Universidade Federal do Maranhão, UFMA, Av. dos Portugueses, 1966 - Vila Bacanga, São Luís, MA 65080-805, Brazil
luisfrp741@gmail.com, {jdallyson,ari}@nca.ufma.br

[2] Núcleo de Computação Aplicada, NCA, Av. dos Portugueses, 1966 - Vila Bacanga, São Luís, MA 65080-805, Brazil

[3] Departamento de Informática, Deinf, Campus Dom Delgado, UFMA, Av. dos Portugueses, 1966 - Vila Bacanga, São Luís, MA 65080-805, Brazil
{paiva,alexandrearaujo,geraldo}@nca.ufma.br

Abstract. Breast cancer is a neoplasm that mainly affects women above the age of 45. However, an increase in the incidence of this disease among young women has been observed. Although it is considered a cancer with a good prognosis when diagnosed early, early detection remains a challenge. In Brazil, the mortality rate due to breast cancer remains high, which is directly related to the late diagnosis of the disease. To contribute to the reduction of this rate, the development of effective early detection techniques is essential. These techniques can assist in diagnosing the disease at its initial stages, enabling quicker treatment and thereby increasing the chances of a cure. Computer-aided detection and diagnosis systems have been developed and improved in the field of computing. These systems base their accuracy and reasoning on data obtained through a combination of computer vision techniques, such as pattern recognition and machine learning. When applied, these techniques assist doctors and specialists in data analysis to provide diagnostic support and treatment planning. This significantly enhances a patient's chances of recovery. More recently, within the machine learning field, Deep Learning has become a prevalent focus of research due to its ability to automatically extract relevant features for the target task. In this work, the methodology proposed employs Convolutional Neural Networks for machine learning. While the results obtained are not superior to those in the literature, they are close and generally require fewer com-

Supported by PIBIC - This work was carried out with the support of the Coordination for the Improvement of Higher Education Personnel - Brazil (CAPES) - Financing Code 001, Maranhão Research Foundation (FAPEMA), National Council for Scientific and Technological Development (CNPq).

A. Cunha et al. (Eds.): MobiHealth 2023, LNICST 578, pp. 223–238, 2024.
https://doi.org/10.1007/978-3-031-60665-6_17

putational resources for training the selected networks after the selection process.

Keywords: Classification · Breast Cancer · Deep Learning

1 Introduction

1.1 Motivation

Cancer is the generic term for a set of more than a hundred diseases that share two basic characteristics: the ability of neoplastic (cancerous) cells to reproduce uncontrollably, forming tumors and potentially invading adjacent organs and tissues, and the ability to spread to distant organs and tissues from the original tumor, a process known as metastasis.

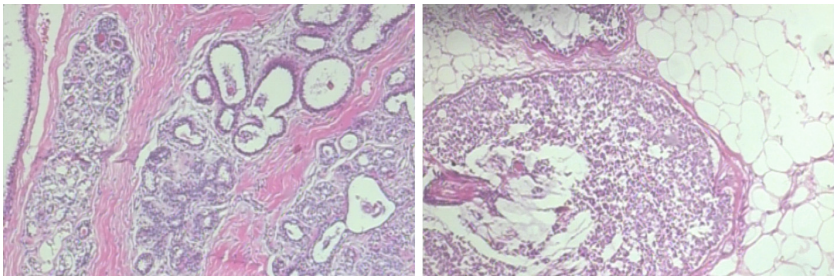

Fig. 1. Image of Benign and Malignant Cancer Cells, adapted from [32]

Breast carcinoma is a diverse disease, displaying wide variation in both its morphological and molecular characteristics, as well as responding variably to clinical treatment [19]. Early diagnosis and timely treatment are essential for a good prognosis and patient recovery. The earlier the diagnosis, the more effective the treatment.

The final diagnosis present in the anatomopathological report is issued by the pathologist through the microscopic analysis of tissue samples obtained by biopsy, also known as histopathological imaging, and additionally, from the surgical specimen. Examples of histopathological images can be seen in Fig. 1. This report should contain essential information, such as the histological subtype and the degree of tumor differentiation [18]. One of the main challenges during the analysis of histopathological examinations is related to the high demand for diagnoses, which is exacerbated by the limited availability of specialized doctors to perform this task. This scenario contributes to delays in diagnoses, as the process requires concentrated effort and can lead to professional fatigue, resulting in potential errors.

Biopsy is a procedure used to acquire histopathological images, and the process involves collecting a tissue sample from the affected area of the breast [4]. Subsequently, this collected sample is carefully examined under a microscope to identify and classify the nature of the tumor. Although it is a relatively invasive procedure, and there are different methods for breast cancer detection, biopsy is the only way to confidently diagnose whether cancer is truly present. For this reason, histopathological diagnosis is considered the gold standard for the clinical diagnosis of cancer [1]. Among biopsy techniques, the most common ones are fine-needle aspiration, core needle biopsy, vacuum-assisted biopsy, and open surgical biopsy (SOB) [32].

1.2 State-of-the-Art

Deep learning is a subfield of artificial intelligence that has revolutionized the ability of machines to learn and understand complex patterns. It utilizes deep neural networks to perform sophisticated tasks in analysis and decision-making. Authors such as Srinidhi et al. [33] and Van der Laak et al. [21] discuss the impact of these techniques and how they have become the most popular area in histopathological image analysis in recent years due to their high capacity for automatic feature extraction. In general, both works categorize deep learning networks based on the type of learning they rely on, which includes supervised learning, weakly supervised learning, unsupervised learning, and transfer learning. In this section, we will focus on supervised learning and transfer learning techniques.

In supervised learning, learning occurs in the form of a function that learns to map an input to an output based on pairs of input-output examples [25]. Typically, classification techniques for this type of learning will either work with classifying patches, small pieces of images, to classify the entire image, or they will work with the whole image for classification. These techniques can range from simple Convolutional Neural Network (CNN) architectures [7] to more complex models [22]. The models traditionally used for image classification can be seen in the field of histopathological images, such as VGGNet [31], InceptionNet [35], ResNet [38], and MobileNet [14].

The main objective of transfer learning is to transfer knowledge from a source domain to a target domain. This strategy relaxes the assumption that the test and training groups must be autonomous and evenly distributed. In the field of histopathology, knowledge transfer is often performed using pre-trained models from the ImageNet dataset, and notable works include [11], [17] and [20].

Several researchers have explored methodologies to enhance feature extraction quality in neural networks. For example, Umer et al. [39] employ transfer learning and machine learning techniques to validate a feature vector. In another study, Ibraheem et al. [16] propose the 3PCNNB-Net, a network comprising three parallel CNN branches designed to optimize information extraction and feature fusion. In Chhipa et al. [5], an unsupervised approach called MPCS is used for representation learning in histopathological images, resulting in high cancer classification accuracy on the BreakHis dataset. In Seo et al. [29], a more image

processing and feature extraction-based approach combined with the Support Vector Machine (SVM) classifier is proposed. The proposed method involves dividing histopathological images into patches, and for each magnification level, Parameter Free Threshold Statistics (PFTS) features are extracted and classified by the pdMISVM (Primal-Dual Multi-Instance Support Vector Machine) classifier. The reported accuracy on the BreakHis dataset in the cited works is respectively 97.14%, 92.70%, 92.15%, and 89.8%.

Finally, Saini et al. [26] propose a Deep Learning architecture involving transfer learning based on VGGNet. The proposed architecture adds dense, batch normalization, dropout, and flattened layers to VGGNet, as well as an Inception block. The network is pre-trained on the ImageNet dataset, and a refinement step, similar to that done by [5], is performed on the BreakHis dataset. The reported accuracy on the dataset is 96.81%.

2 Deep Learning Models

In this section, we will briefly discuss the architectures that have achieved the best performance in the proposed methodology. MobileNetV2 [27] is an evolution of the MobileNet architecture [14], improved for better efficiency and representation capacity. It introduces enhancements such as the Bottleneck Residual Block, inspired by ResNet [12], which captures residual information, and the Inverted Residual Blocks, which effectively expand and reduce the dimensions of intermediate representations, as seen in Fig. 2.

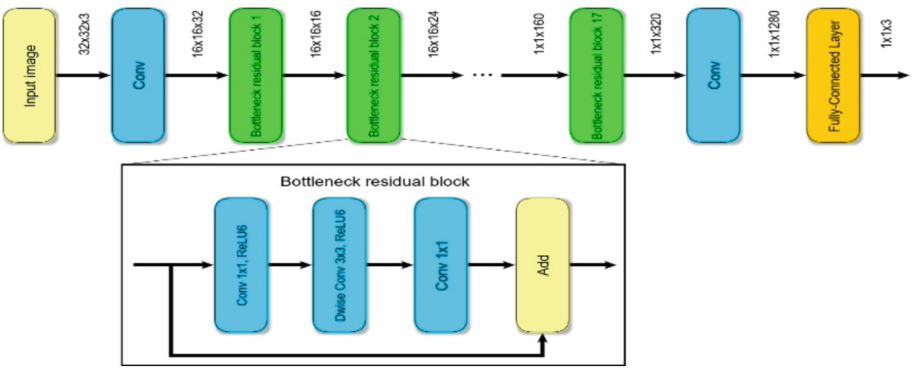

Fig. 2. Architecture of mobileNetV2 adapted from [28].

The network also uses Linear Bottleneck layers to increase flexibility and nonlinearity, along with Squeeze and Excitation (SE) Activation Filters, which are used to enhance crucial information by modeling dependencies between feature channels.

The central idea of EfficientNetV2 [37] is to improve training speed while maintaining parameter efficiency, which is associated with the ability to achieve

good results with a smaller number of parameters. The EfficientNetV2 introduces several modifications compared to EfficientNet [36], as seen in Fig. 3, including the use of new types of blocks, a combination of MBconv and fused-MBConv [10] adjustments in expansion rates and kernel sizes, and the removal of the stride-1 step. These changes are made to enhance the efficiency and performance of the architecture [37]. We can see the structure of MBConv and FusedConv in Fig. 4.

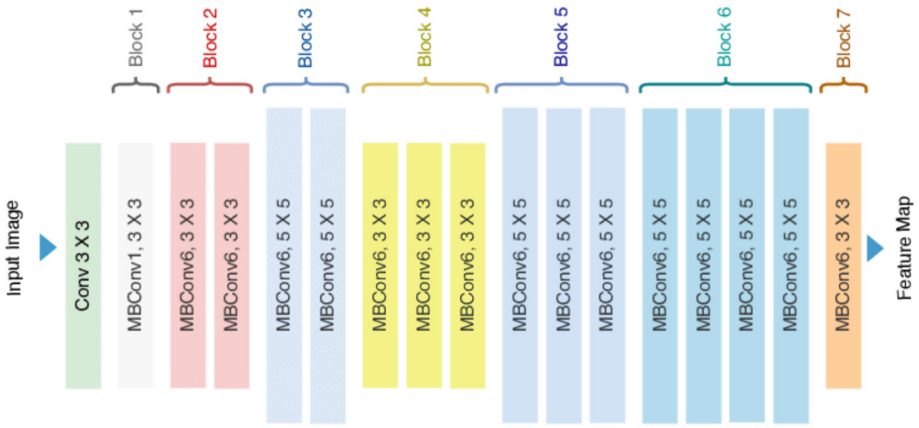

Fig. 3. Architecture of EfficientNet-B0 with MBConv as Basic building blocks, adapted from [2].

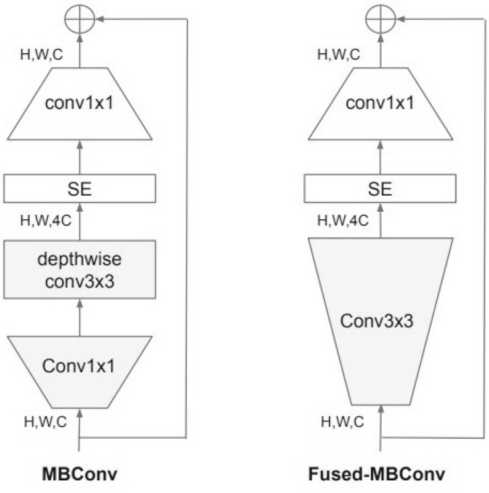

Fig. 4. Architecture of MBConv and FusedConv, adapted from [37].

Inception-v3 [34] is a variant of Inception-v2 that incorporates the concept of BN-auxiliary. This term refers to the version where the fully connected layer of the auxiliary classifier is also normalized, extending beyond just the convolutions. In this context, the combination of Inception-v2 with BN-auxiliary is called Inception-v3, representing an evolution in the original architecture. Additionally, Inception-v3 also incorporates the idea of Reduction Modules between these Inception modules. The reduction modules employ larger convolutions, such as 3×3 with increased stride, followed by 1×1 convolutions, to reduce the dimensionality of representations and increase computational efficiency. You can see the network diagram in Fig. 5.

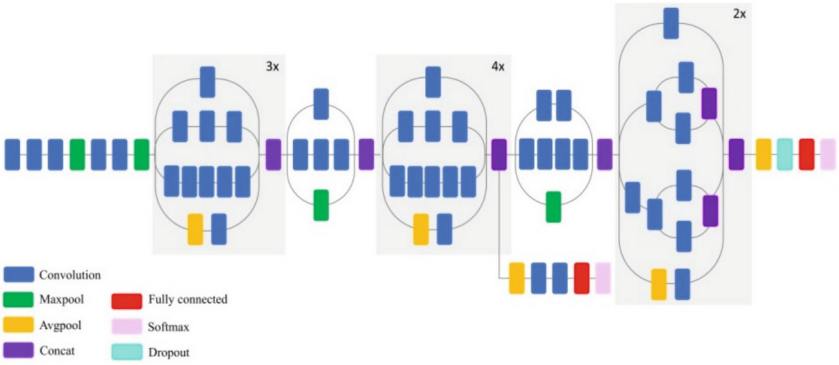

Fig. 5. Schematic diagram of InceptionV3 model, adapted from [23].

3 Materials and Methods

The flowchart of this work is illustrated in Fig. 6, which will be explained in more detail in this section. In summary, starting from the BreakHis dataset, which contains breast tissue images for lesion classification, preprocessing procedures were performed on the images before splitting them into training, testing, and validation sets. These sets were used to train and evaluate the different models.

3.1 Dataset BreakHis

For this work, the BreakHis dataset was used, which contains 7,909 histopathological images acquired from 82 patients using different magnification factors (40X, 100X, 200X, and 400X). Out of these images, 2,480 are benign samples, and 5,429 are malignant samples. The images were collected using the SOB method, have a resolution of 700×460 pixels, and consist of 3 channels of 8-bit color (RGB). A complete description of the sample count for each magnification level in the dataset can be seen in Table 1. The associated task with this dataset is the automated classification of these images [32].

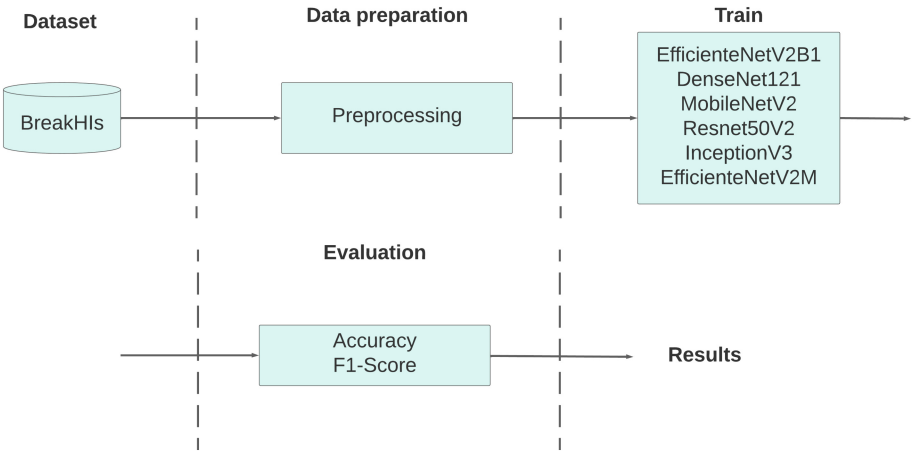

Fig. 6. Pipeline of the developed work.

Table 1. Description of the number of images in the BreakHis dataset by classes and magnification, adapted from [32]

Magnification	Benign	Malignant	Total
40X	652	1,370	1,995
100X	644	1,437	2,081
200X	623	1,390	2,013
400X	588	1,232	1,820
Total number of images	2,480	5,429	7,909

3.2 Data Preparation

In the preprocessing step of the images, data augmentation techniques were used, applying various transformations to each training instance while preserving the relationship with the annotations, with the aim of artificially expanding the amount of information for improved network learning [24].

The techniques applied for data augmentation were: Horizontal Flip, used to horizontally flip the image; Vertical Flip, used to vertically flip the image; Rotation, used to rotate the image; and Brightness, responsible for adjusting the brightness level in the images. All data augmentation techniques were conditioned to a factor of 0.2.

To reduce discrepancies among various images, a technique known as stain normalization [8] essentially transfers the average color from the source of one image to other images. Although deep learning (DL) algorithms may be able to partially reduce color variations through data augmentation, the performance of the results deteriorates due to the limited amount of data.

In this work, the stain normalization technique was adopted to reduce the color variability in histopathological images, establishing a standard, thereby facilitating model learning. Additionally, the image size of 460×700 was resized to the standard 224×224.

3.3 Training

After completing the preprocessing step of the images using stain normalization and data augmentation techniques,

Table 2. Results obtained using transfer learning and stain normalization.

Model	Accuracy	F1-Score
EfficienteNetV2B1	0,8581	0,8971
DenseNet121	0,8551	0,8940
MobileNetV2	0,8739	0,9090
Resnet50V2	0,8406	0,8877
InceptionResNetV2	0,8365	0,8846
InceptionV3	0,8710	0,9067
VGG16	0,7994	0,8564
EfficientNetV2M	0,8427	0,8852

The fitness function is responsible for evaluating the performance of a neural network with the aim of enhancing and seeking an improvement in results with each generation [30]. For this work, the optimizer used was Adam with a learning rate of 5e-4. The loss function employed was BinaryCrossentropy, which aims to minimize the discrepancies towards the desired class value. Training was conducted for 100 epochs, and the networks used were Resnet50V2 [13], DenseNet121 [15], MobileNetV2 [27], VGG16 [31], InceptionResNetV2 [34], InceptionV3 [35], EfficienteNetV2B1 [37] and EfficientNetV2M [37].

After training all the networks, the top 3 networks with the highest accuracy were selected, as shown in Table 2. This allowed for the selection of the network ensemble that will be used in the next phase.

Ensemble. Ensemble learning [40] is a method in which multiple models are combined to enhance the performance of a final model in machine learning tasks. Ensemble methods provide a powerful way to improve the generalization capability and accuracy of machine learning models. For the purpose of this binary classification task, the adopted method was voting, as it is the most common and yields good results [40].

Voting is a common method of combination, which can be implemented in various ways, including majority voting. Thus, majority voting is a method of

combining predictions from multiple base models in an ensemble. Majority voting counts how many models predict each class and then makes the final prediction based on the class that receives the majority of votes [9].

After selecting the three networks with the best performance, we combined their predictions using a voting approach. Since we are dealing with a binary classification task where classes are represented as 0 (benign) or 1 (malignant), we applied the following criterion: if a class received an equal or greater number of votes than 2, it is considered to belong to the malignant class; otherwise, if it received 1 vote or none, it is classified as benign. This process results in the creation of an array of consolidated predictions through this voting process.

3.4 Evaluation

In this section, we will discuss the definition of the metric used in this work: Accuracy and F1-Score.

Accuracy is the ratio of the number of correctly classified samples to the total number of samples. We can understand it as follows, as per Eq. 1: True Positive (TP) represents the number of true positive cases. True Negative (TN) is the number of true negative cases. False Positive (FP) is the number of false positives, and False Negative (FN) is the number of false negatives. All of these values are derived from the confusion matrix [6].

$$acc = \frac{TP + TN}{TP + TN + FP + FN} \tag{1}$$

The F1-Score is the harmonic mean of Precision and Recall [6], as seen in Eq. 2. Therefore, when the F1-Score is low, it indicates that either Precision or Recall is low.

$$f1 = 2\frac{precision \times recall}{precision + recall} \tag{2}$$

Recall is the number of relevant items retrieved as a proportion of all relevant items [3]. We can describe Recall as the ratio of the number of true positives to the sum of true positives and false negatives. In this way, Recall is used to assess the percentage of data classified as positive compared to the actual quantity of positives in the sample [3].

$$recall = \frac{TP}{TP + FN} \tag{3}$$

Precision is a measure of purity used to assess the performance of Recall, as it gauges the effectiveness in excluding irrelevant items from the retrieved set. Therefore, both high Precision and high Recall are desirable [3].

$$precision = \frac{TP}{TP + FP} \tag{4}$$

4 Results

In this section, the results obtained in different experiments will be presented. Additionally, the evaluations were conducted using accuracy as the metric.

Table 3. Results obtained with the original dataset.

Model	Accuracy	F1-Score
EfficienteNetV2B1	0,8177	0,8756
DenseNet121	0,8023	0,8629
MobileNetV2	0,7965	0,8563
ResNet50V2	0,7827	0,8464
InceptionResNetV2	0,6987	0,8226
InceptionV3	0,6987	0,8226
VGG16	0,7827	0,8464
EfficientNetV2M	0,7553	0,8354

When conducting tests with the original dataset, we observed that the EfficientNetV2B1 network demonstrated superior performance compared to other architectures, as highlighted in Table 3. Therefore, we chose to use this network to obtain the images that will be used as a reference when applying the stain normalization technique. To do this, we analyze the predictions in the training set, prioritizing those with the highest associated confidence. This procedure allows us to identify which malignant or benign images contributed most significantly to the learning of the neural network.

Table 4. Results of the accuracies obtained using benign and malignant targets.

Model	Target benign	Target malignant
EfficienteNetV2B1	0,8054	0,8581
DenseNet121	0,8410	0,8551
MobileNetV2	0,8280	0,8739
Resnet50V2	0,8236	0,8406
InceptionResNetV2	0,8262	0,8365
InceptionV3	0,8245	0,8710
VGG16	0,7072	0,7072
EfficientNetV2M	0,8315	0,8427

After selecting the benign image with the best performance and the malignant image, we conducted an additional experiment to assess which of the two

would stand out after being subjected to the stain normalization process, as shown in Table 4. Due to the substantial computational cost associated with training on the complete image set, the decision was made to exclusively train using magnifications of 200x and 400x. In this context, the training set consisted of a total of 2,682 images, with 804 images allocated for validation purposes (30%), 1,878 images for the actual training (70%), and finally, 1,151 images for the test set.

Table 5. Comparison of the accuracies obtained using stain normalization alone and using stain normalization with transfer learning.

Model	Stain Normalization	Stain Normalization + Transfer Learning
EfficienteNetV2B1	0,7611	0,8581
DenseNet121	0,6987	0,8551
MobileNetV2	0,6987	0,8739
Resnet50V2	0,7499	0,8426
InceptionResNetV2	0,6987	0,8365
InceptionV3	0,6987	0,8710
VGG16	0,6987	0,6987
EfficientNetV2M	0,7387	0,8427

After verifying that using the malignant image as a reference for stain normalization in the dataset, along with techniques like data augmentation and transfer learning, resulted in improved model performance, we expanded this approach to the entire set of images. We can observe how the use of transfer learning affected the learning of the networks, as seen in Table 5. Additionally, data augmentation was applied in both experiments.

Table 6. Result obtained and compared to the literature.

Method	Accuracy	F1-Score
pdMISVM [29]	0,8960	0,9112
Feature-level fusion-based FS framework [39]	0,9270	–
MPC [5]	0,9223	–
3PCNNB [16]	0,9180	–
VGG16 Modified with Inception block and dense layer [26]	0,9681	0,9387
Proposed	0,8847	0,9169

When analyzing Table 6, it becomes evident that the proposed methodology did not manage to surpass the accuracy of the works in the same area. However, it

is crucial to highlight that all of these methods employ custom feature extraction processes, as mentioned in [29]. Furthermore, although the computational cost for training the complete set of networks to select the top three was higher compared to the analyzed works, the total training cost for these three top-performing networks ends up being lower than that of the compared works.

This occurs, in part, due to the lower complexity of the chosen networks compared to those mentioned in [31] and [26], which have a higher number of parameters. This difference in the number of parameters may require more substantial computational resources and can lead to overfitting issues.

In this study, the networks selected for the ensemble were InceptionV3, MobileNetV2, and EfficientNetV2B1, containing 23.9, 3.5, and 8.2 million parameters, respectively, totaling 38.8 million parameters. This approach of combining models aims to explore their complementarities and mitigate their individual limitations, thereby seeking a more robust result.

5 Discussion

Overall, the results obtained individually by the top three networks are quite similar. However, when we employ the voting technique, we can observe a modest improvement in the model's accuracy. Below, we present the model's predictions based on a small sample of the test set, as illustrated in Fig. 7.

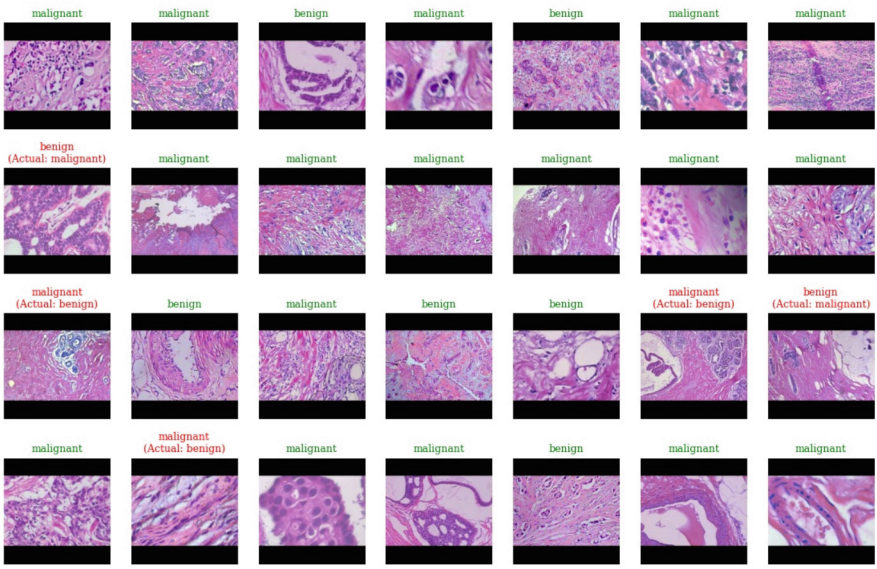

Fig. 7. Predictions of the proposed method

We can also analyze the results from the perspective of the confusion matrix, which provides a visualization of the balance between correct predictions and errors of the final model, as demonstrated in the Fig. 8.

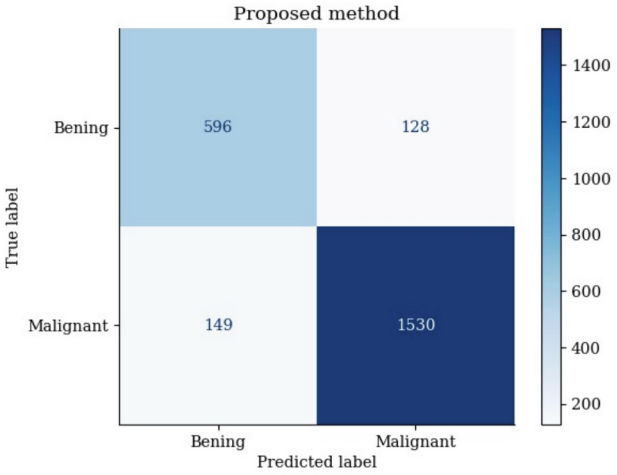

Fig. 8. Confusion matrix of the proposed method

When examining the confusion matrix, we notice that despite the imbalance present in the dataset, we were able to achieve a satisfactory number of correct predictions. Out of the 724 benign images in the set, the model correctly predicted 596, which corresponds to an accuracy rate of approximately 82%. Regarding the 1679 malignant images, the model correctly predicted 1530, resulting in an accuracy rate of around 91%.

These results demonstrate the model's ability to make accurate predictions, even in a scenario where the classes are unbalanced.

6 Conclusion

The improvement in disease detection in breast tissue through feature extraction and computational methods for the analysis of histopathological exams, using image processing, is of fundamental importance for both physicians and patients. This study presents the development of an image classification method using machine learning techniques, specifically in the field of Deep Learning, for the detection of breast cancer in histopathological images. Although the proposed methodology did not manage to surpass the accuracy of works in the same area, the results obtained are satisfactory, even when compared to the literature. The computational cost for training the complete set of networks to select the top 3 is higher compared to the analyzed works. However, the training of the top 3 networks ends up being more cost-effective than in the comparative works.

The study employs InceptionV3, MobileNetV2, and EfficientNetV2B1 in the ensemble, totaling 38.8 million parameters.

References

1. Aeffner, F., et al.: The gold standard paradox in digital image analysis: manual versus automated scoring as ground truth. Arch. Pathol. Lab. Med. **141**(9), 1267–1275 (2017)
2. Ahmed, T., Sabab, N.: Classification and understanding of cloud structures via satellite images with EfficientUNet (2020). https://doi.org/10.1002/essoar.10507423.1
3. Buckland, M., Gey, F.: The relationship between recall and precision. J. Am. Soc. Inf. Sci. **45**(1), 12–19 (1994)
4. Chekkoury, A., et al.: Automated malignancy detection in breast histopathological images. In: Medical Imaging 2012: Computer-Aided Diagnosis, vol. 8315, pp. 332–344. SPIE (2012)
5. Chhipa, P.C., Upadhyay, R., Pihlgren, G.G., Saini, R., Uchida, S., Liwicki, M.: Magnification prior: a self-supervised method for learning representations on breast cancer histopathological images. arXiv preprint: arXiv:2203.07707 (2022)
6. Chicco, D., Jurman, G.: The advantages of the Matthews correlation coefficient (MCC) over F1 score and accuracy in binary classification evaluation. BMC Genomics **21**(1), 1–13 (2020)
7. Cruz-Roa, A., et al.: Automatic detection of invasive ductal carcinoma in whole slide images with convolutional neural networks. In: Medical Imaging 2014: Digital Pathology, vol. 9041, p. 904103. SPIE (2014)
8. Deng, S., et al.: Deep learning in digital pathology image analysis: a survey. Front. Med. **14**, 470–487 (2020)
9. Ganaie, M.A., Hu, M., Malik, A., Tanveer, M., Suganthan, P.: Ensemble deep learning: a review. Eng. Appl. Artif. Intell. **115**, 105151 (2022)
10. Gupta, S., Tan, M.: Efficientnet-EdgeTPU: creating accelerator-optimized neural networks with AutoML. Google AI Blog **2**(1) (2019)
11. Hassan, A.M., El-Mashade, M.B., Aboshosha, A.: Deep learning for cancer tumor classification using transfer learning and feature concatenation. Int. J. Electr. Comput. Eng. **12**(6), 6736 (2022)
12. He, K., Zhang, X., Ren, S., Sun, J.: Deep residual learning for image recognition. In: Proceedings of the IEEE Conference on Computer Vision and Pattern Recognition, pp. 770–778 (2016)
13. He, K., Zhang, X., Ren, S., Sun, J.: Identity mappings in deep residual networks (2016)
14. Howard, A.G., et al.: MobileNets: efficient convolutional neural networks for mobile vision applications. arXiv preprint: arXiv:1704.04861 (2017)
15. Huang, G., Liu, Z., van der Maaten, L., Weinberger, K.Q.: Densely connected convolutional networks (2018)
16. Ibraheem, A.M., Rahouma, K.H., Hamed, H.F.: 3pcnnb-net: Three parallel CNN branches for breast cancer classification through histopathological images. J. Med. Bio. Eng. **41**(4), 494–503 (2021)
17. Ijaz, A., et al.: Modality specific CBAM-VGGNet model for the classification of breast histopathology images via transfer learning. IEEE Access **11**, 15750–15762 (2023)

18. INCA: Estimativa 2020, incidência de câncer no brasil (2020). https://www.inca.gov.br/estimativa/introducao#:~:text=Nas%20mulheres%2C%20exceto%20o%20c%C3%A2ncer,%25
19. INCA: Detecção precoce do câncer (2021b), referência completa: *Instituto Nacional de Câncer José Alencar Gomes da Silva. Detecção precoce do câncer*. Rio de Janeiro: INCA, 2021b. Disponível em: https://www.inca.gov.br/publicacoes/livros/deteccao-precoce-do-cancer. Acesso em: 16 ago. 2023
20. Joshi, S.A., Bongale, A.M., Olsson, P.O., Urolagin, S., Dharrao, D., Bongale, A.: Enhanced pre-trained Xception model transfer learned for breast cancer detection. Computation **11**(3), 59 (2023)
21. Van der Laak, J., Litjens, G., Ciompi, F.: Deep learning in histopathology: the path to the clinic. Nat. Med. **27**(5), 775–784 (2021)
22. Liu, J., et al.: An end-to-end deep learning histochemical scoring system for breast cancer TMA. IEEE Trans. Med. Imaging **38**(2), 617–628 (2018)
23. Mahdianpari, M., Salehi, B., Rezaee, M., Mohammadimanesh, F., Zhang, Y.: Very deep convolutional neural networks for complex land cover mapping using multispectral remote sensing imagery. Remote Sens. **10**(7), 1119 (2018)
24. Pérez-García, F., Sparks, R., Ourselin, S.: Torchio: A python library for efficient loading, preprocessing, augmentation and patch-based sampling of medical images in deep learning. Comput. Methods Programs Biomed. **208**, 106236 (2021). https://doi.org/10.1016/j.cmpb.2021.106236, https://www.sciencedirect.com/science/article/pii/S0169260721003102
25. Russell, S.J.: Artificial Intelligence a Modern Approach. Pearson Education Inc., London (2010)
26. Saini, M., Susan, S.: VGGIN-Net: deep transfer network for imbalanced breast cancer dataset. IEEE/ACM Trans. Comput. Biol. Bioinform. **20**, 752–762 (2022)
27. Sandler, M., Howard, A., Zhu, M., Zhmoginov, A., Chen, L.C.: MobileNetV2: inverted residuals and linear bottlenecks. In: Proceedings of the IEEE Conference on Computer Vision and Pattern Recognition, pp. 4510–4520 (2018)
28. Seidaliyeva, U., Akhmetov, D., Ilipbayeva, L., Matson, E.: Real-time and accurate drone detection in a video with a static background. Sensors **20**, 3856 (2020). https://doi.org/10.3390/s20143856
29. Seo, H., Brand, L., Barco, L.S., Wang, H.: Scaling multi-instance support vector machine to breast cancer detection on the BreaKHis dataset. Bioinformatics **38**(Supplement_1), i92–i100 (2022)
30. Silva, D.A., et al.: Otimização da função de fitness para a evolução de redes neurais com o uso de análise envoltória de dados aplicada à previsão de séries temporais (2011)
31. Simonyan, K., Zisserman, A.: Very deep convolutional networks for large-scale image recognition. arXiv preprint: arXiv:1409.1556 (2015)
32. Spanhol, F.A., Oliveira, L.S., Petitjean, C., Heutte, L.: A dataset for breast cancer histopathological image classification. IEEE Trans. Biomed. Eng. **63**(7), 1455–1462 (2016). https://doi.org/10.1109/TBME.2015.2496264
33. Srinidhi, C.L., Ciga, O., Martel, A.L.: Deep neural network models for computational histopathology: a survey. Med. Image Anal. **67**, 101813 (2021)
34. Szegedy, C., Ioffe, S., Vanhoucke, V., Alemi, A.: Inception-v4, inception-ResNet and the impact of residual connections on learning (2016)
35. Szegedy, C., Vanhoucke, V., Ioffe, S., Shlens, J., Wojna, Z.: Rethinking the inception architecture for computer vision. In: Proceedings of the IEEE Conference on Computer Vision and Pattern Recognition, pp. 2818–2826 (2015)

36. Tan, M., Le, Q.: EfficientNet: rethinking model scaling for convolutional neural networks. In: International Conference on Machine Learning, pp. 6105–6114. PMLR (2019)
37. Tan, M., Le, Q.V.: EfficientNetV2: smaller models and faster training (2021)
38. Targ, S., Almeida, D., Lyman, K.: ResNet in ResNet: generalizing residual architectures. arXiv preprint: arXiv:1603.08029 (2016)
39. Umer, M.J., Sharif, M., Alhaisoni, M., Tariq, U., Kim, Y.J., Chang, B.: A framework of deep learning and selection-based breast cancer detection from histopathology images. Comput. Syst. Sci. Eng. **45**(2) (2023)
40. Zheng, Y., et al.: Application of transfer learning and ensemble learning in image-level classification for breast histopathology. Intell. Med. **3**(02), 115–128 (2023)